JCTC Journal of Chemical Theory and Computation

Quantum Mechanics/Molecular Mechanics Calculations of the Vanadium Dependent Chloroperoxidase

Joslyn Yudenfreund Kravitz,[†] Vincent L. Pecoraro,[†] and Heather A. Carlson*[,†,‡]

Department of Chemistry, University of Michigan, Ann Arbor, Michigan 48109-1055, and Department of Medicinal Chemistry, College of Pharmacy, University of Michigan, Ann Arbor, Michigan 48109-1065

Received May 13, 2005

Abstract: Large quantum mechanics/molecular mechanics (QM/MM) calculations are used to probe the resting and initial protonated states of the vanadium dependent chloroperoxidase from the pathogenic fungus *Curvularia inaequalis.* QSite was used to model 433 residues and 24 structural waters with molecular mechanics, while 8 active-site residues and the vanadate cofactor (161 atoms) were represented at the B3LYP/lacvp* level of theory. Our previous study of small model systems implied that the resting state of the enzyme contains a trigonal bipyramidal vanadate with one hydroxyl group in the equatorial plane and another in the axial position. This study uses a much larger model of the biological system at a higher level of theory to identify the location of the equatorial hydroxo group with respect to the enzyme active site. We also identify a second resting-state configuration with an axial water and three equatorial oxo moieties that is nearly isoenergetic with the previously identified state. We propose that the resting state is a hybrid of these two configurations, stabilized by the long-range electrostatic field of the protein environment. The first step in catalysis is believed to be protonation of the vanadate. Our previous small models indicated that there were two protonated configurations, but this study shows that the configuration containing an axial water and one hydroxo group in the equatorial plane is significantly lower in energy than any other configuration. Additionally, we can now assign an important role for lysine 353 in the catalytic cycle. Based on our calculations and other model studies, we provide an updated catalytic cycle for vanadium dependent haloperoxidase activity. Further, we demonstrate the importance of system set up. In particular, maintaining the proper electrostatic field at the active site is crucial for identifying the correct minima in a truncated protein model.

Introduction

Recent computational studies have resulted in new proposals for the structure[1] and catalytic reactivity[2] of the active site of the vanadium dependent haloperoxidases. These unusual enzymes catalyze the two electron conversion of halide ions to the corresponding hypohalous acids using hydrogen peroxide as an oxidant:[3]

$$H_2O_2 + H^+ + X^- \rightarrow H_2O + \text{“HOX”} \qquad (1)$$

Chloride, bromide, or iodide can be used as substrate for a vanadium dependent chloroperoxidase (VCPO), but only bromide and iodide can be oxidized by vanadium dependent bromoperoxidases (VBPO). The identity of “HOX” is dependent upon both the pH of the reaction and the halide involved. Studies indicate that VCPO oxidizes a chloride ion

* Corresponding author e-mail: carlsonh@umich.edu.
[†] Department of Chemistry.
[‡] Department of Medicinal Chemistry, College of Pharmacy.

10.1021/ct050132o CCC: $30.25
Published on Web 09/20/2005

to HOCl,[4] whereas the products of bromide oxidation are likely a thermodynamic distribution of Br_3^-, HOBr, and Br_2.[5]

Unlike heme-based peroxidases, which require the formation of highly oxidized intermediates, the vanadium does not undergo redox cycling during catalysis. It is thus believed that the vanadium ion plays the role of a strong Lewis acid which activates the peroxide.[6] Kinetic studies indicated that protonation of the bound peroxo group is a crucial step in the heterolytic cleavage of the O−O bond. These observations formed the basis for a proposal that the protonated oxygen is then transferred to the halide according to an oxo-transfer mechanism.[7] Subsequent computational studies now suggest that the nonprotonated peroxo oxygen is the atom transferred to the substrate.[2]

Upon oxidation, the halide can be added to an organic substrate if one is present.[8] In some cases, this addition is stereoselective.[9] This reaction is thought to be the origin of many halogenated species in the environment.[10] In fact, Butler and co-workers recently carried out the first experiments which established the role of these enzymes in the biosynthesis of brominated metabolites from marine red algae.[11] At high pH and in the absence of organic substrate, the oxidized halogen can react with a second equivalent of peroxide to produce singlet oxygen.[12] Additionally, VBPOs can oxidize thioethers to the corresponding sulfoxide[13] using a mechanism similar to that of halide oxidation.[14]

Peroxo−vanadium complexes are good functional models of the VCPO and have been shown to oxidize organic[15] and inorganic compounds,[16] including alcohols[17] and sulfides.[14] They are also capable of hydroxylating hydrocarbons[18] and epoxidizing alkenes.[19] However, attempts to synthesize structural models of the VCPO active site have not been as successful, and a synthetic complex reproducing the exact coordination environment of vanadium in VCPO has not yet been obtained. It has been proposed that such a complex has not been isolated because a five-coordinate imidazole complex is unstable unless sequestered in a protein active site.[20]

The only crystal structure of a VCPO that has been solved is the enzyme from the fungus *Curvularia inaequalis*.[21] In the native state, the vanadate cofactor (VO_4^{3-}) is bound to the protein through a single coordinate covalent bond from the V to the N_ϵ of His496 (Figure 1). The high negative charge of the cofactor appears to be offset by a number of protonated amino acids in the active site which donate hydrogen bonds to the oxygen atoms of the cofactor (Lys353, Arg360, and Arg490). Additional hydrogen bonds are donated to vanadate's equatorial oxygens by the side chain of Ser402 and the backbone amide of Gly403. His404 may participate in a hydrogen bond to or from an axial hydroxo group.

Mutagenesis studies[22] in which each of the three basic active-site residues and His496 were replaced with alanine indicated that His496 and Lys353 are the two most important residues for activity. Replacement of Arg490 or Arg360 leads to a lesser, but still significant, reduction in activity. Additional mutants which eliminate almost all activity are His404, which is involved in a hydrogen bond with the axial oxygen moiety, and Asp292, which helps orients Arg490 through a strong salt bridge.[23]

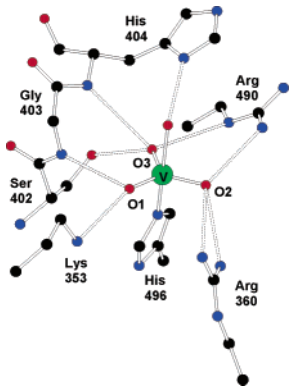

Figure 1. Active site configuration observed in the crystal structure of the VCPO from *C. inaequalis*.[1] The hydrogen-bonding interactions shown above are implied from distances between the heavy atoms. The equatorial oxygens of the vanadate are labeled with the notation used throughout our discussions.

The crystal structure of this enzyme was interpreted to contain a vanadate unit in a trigonal bipyramidal structure with a hydroxide and His496 in the axial positions and three oxo moieties in the equatorial plane. However, due to inherent limitations in resolution, the crystallographic study did not reveal hydrogen positions, and the distinction between oxide and hydroxide moieties was inferred by slight differences in ligand−metal bond distances which were less than the uncertainty in the atomic positions.

Computational studies of this enzyme complement and correlate well to available experimental techniques. Michael Bühl and co-workers have carried out an extensive series of DFT calculations in which ^{51}V NMR chemical shift values were calculated.[24−27] Valeria Conte and co-workers have carried out calculations for small models of each catalytic intermediate. These calculations, done on vanadate models of fewer than 10 atoms, provided some insight into the order and location of peroxide[28] and bromide binding[29] and reactivity.[30] More recent studies, carried out by De Gioia and co-workers,[2] involved slightly larger models of the active site, incorporating methylamine and imidazole moieties to represent Lys353 and His496. This study examined models of each catalytic intermediate in the cycle.

The conclusions from these studies agree well with our recent studies of small models to represent the active site of both the VCPOs and VBPOs. These calculations revealed that the resting state of the enzyme included an anionic, doubly protonated vanadate.[1] In this species, the axial position and one equatorial position were protonated, while the other two equatorial positions contained oxo moieties. This is slightly different than the proposed active site based on the crystal structure of the VCPO where it was suggested that three oxo groups were found in the equatorial plane.[31] Based on the atomic arrangement of the peroxide-bound crystal structure, it was proposed that the axial hydroxo group is protonated and then leaves as water.[21] This is consistent with our calculations which showed that the energy difference between protonation of either the axial hydroxo or one

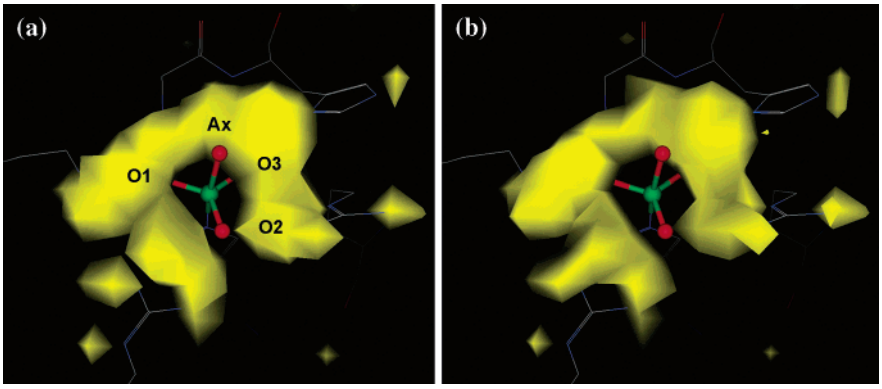

Figure 2. An electrostatic isosurface in the active site calculated for (a) the full chloroperoxidase and (b) the truncated protein model. The isosurfaces pictured here represent only the protein's contribution to the electric field (vanadate not included in the calculation). The isosurface is shown at 8 kT for the full protein and 9 kT for the truncated protein.

equatorial oxo moieties was negligible, indicating that either could be the site of the protonation that begins the catalytic cycle. From our previous model calculations, it is clear that the structure and stability of the vanadate cofactor is highly dependent upon the hydrogen-bonding partners available to the various oxygen ligands. To characterize the active site of the enzyme fully, a larger system with a complete active site is needed.

This paper presents a hybrid quantum mechanics/molecular mechanics (QM/MM) study of the resting and first protonation states of the VCPO from the fungus *C. inaequalis*. This computational method treats part of the protein quantum mechanically (the vanadate cofactor and selected surrounding residues), while the remainder of the protein is treated using molecular mechanics. In this way, a high level electronic calculation of the active site can be carried out in the presence of the actual protein environment. In our application of this powerful new technique, we were able to use a quantum mechanical region of 161 atoms (with 42 additional interface atoms), making this one of the largest, high-accuracy QM/MM calculations to date. Our application also highlights the need for careful attention to long-range, electrostatic interactions provided by the protein environment.

Computational Methods

Friesner and co-workers have developed QSite,[32−34] a QM/MM program well suited to study metalloenzymes. They have shown that the binding energy of O_2 to hemerythrin[35] and the activation barrier in cytochrome P450cam hydrogen abstraction[36] could be calculated quite accurately using this program. Unless noted, all of our calculations were carried using QSite version 2.5, revision 20.[37] QM/MM calculations were completed with the default parameters in QSite, including the OPLS 1999 force field[38] and a distance-dependent dielectric constant. We used the B3LYP[39,40] functional with the lacvp* basis set which uses the Los Alamos ECP including the outermost core orbitals[41] for vanadium and 6-31G*[42−47] for all other atoms. In all calculations, backbone atoms were held fixed. Any residues more than 20 Å from the vanadium were also held fixed (including protons).

Protein Preparation. Using the program Maestro, the atoms of the side chains of six residues that were unresolved in the crystal structure (PDB code 1VNI)[21] were added. Prolines 361 and 401 were converted to alanines because of software limitations in the QM/MM interface region (backbone atoms were constrained to the positions in the crystal structure, so this change is minimal). Protons were added and oriented to maximize the hydrogen-bonding network within the protein using the program MOE.[48]

While QSite allows a maximum of 8000 atoms and bonds in the system, the chloroperoxidase is comprised of over 9000 atoms. To deal with the size limitation, the protein had to be truncated by removing sections that were distant from the vanadate cofactor. We cannot overemphasize how important it is to maintain the electrostatic field in the active site when creating a truncated model. It was important to choose distant residues that would have less effect on the electrostatics at the active site. The chloroperoxidase has an overall charge of −26, and careful choices were made to minimize any disruption of the electric field at the active site. Thus, the electric field of the entire protein and that of several potential truncation models were calculated using the Poisson−Boltzmann routine in the program MOE. The field of the protein alone was calculated to determine the environment with which the vanadate cofactor will interact. It was necessary to identify which truncated model best reproduced the field of the whole protein. The parameters used in the calculation were as follows: the dielectric constant of the interior of the protein was set to 20; the dielectric constant for the exterior of the protein was set to 80; offset was 2 Å; the counterion and solvent radii were 2.5 and 1.4 Å, respectively; the grid spacing was 1 Å and the grid extended 20 Å beyond the protein; the salt (NaCl) and solute (protein) concentrations were 0.15 M and 0.001 M, respectively. The appropriate truncated system was chosen based on its ability to most closely reproduce the field of the whole protein at the active site (Figure 2). Though it was not possible to maintain the magnitude of the field when eliminating so many charges, it was possible to maintain the topography of the field. This produces the same gradients, so the relative effect on the wave functions will be the same. Protonation biases will also be as similar as possible.

The truncation model which yielded the best result was based on an approximate 27-Å cutoff from the vanadate. To maintain the electrostatic characteristic of the protein envi-

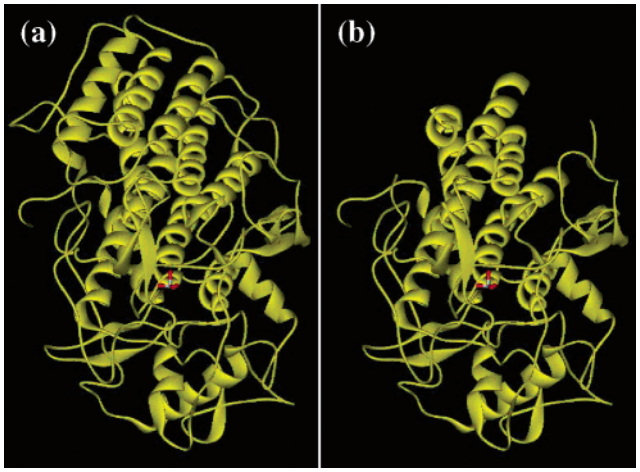

Figure 3. (a) The complete chloroperoxidase and (b) the truncated model used in this study. Vanadate is shown in ball-and-stick representation, roughly at the center of both structures.

ronment, the charges of the residues at the cutoff distance were considered when choosing which residues to remove. For instance, neutral residues were cut preferentially over charged ones. In cases where a charged residue near the cutoff was part of a salt bridge, both residues were removed. At a distance greater than 25 Å, a salt bridge has an electrostatic effect similar to a neutral dipole. All chains that were cut were capped with *N*-methylamide (NME) or acetyl (ACE) residues as appropriate (Figure 3). A list of the residues which were included in the truncated model of the protein is available in the Supporting Information. Surface water molecules were removed, but structural waters in the interior were retained. This procedure resulted in a careful pruning of the protein to contain 7018 atoms with an overall charge of −14 and an appropriate electric field gradient in the active site.

The positions of all protons were minimized using Impact version 2.5 revision 20.[49]

Definition of Quantum Mechanics Region. As in our previous study, our investigation proceeded by building up the QM region in a systematic fashion starting from a dianionic vanadate. In all calculations, the vanadate group and the side chain of His496 were included in the QM region. The initial calculations used a QM region that also included Lys353, Arg360, and Arg490. This QM region had a total charge of +1 and contained 113 lacvp* atoms with 28 additional interfacial atoms (four residue calculations). A second set of calculations included the same four residues plus the side chains of Asp292 and His404 in the QM region (six residue calculations). The QM region was net neutral in charge and contained 138 lacvp* atoms with 36 interface atoms. A final set of calculations for the anionic resting state of the protein was carried out in which a proton was added to the system in all possible locations (full resting state calculations). These calculations also included the backbone of His404 and all of Gly403 in the QM region. The first protonation step in the catalytic cycle was generated by again adding a proton to all appropriate locations in the active site (first protonation state calculations). The full resting state and first protonation state calculations contained 160 and 161 lacvp*atoms in the QM region, respectively, with 42 interfacial atoms (a total of 202 and 203 atoms in the largest calculations). The QM region had a net charge of +1 for the full resting state and +2 for the first protonation state (Figure 4).

In the four residue calculations, the heavy atoms of all QM side chains were frozen, but the vanadate atoms and all QM protons were allowed to move. For all other calculations, vanadate and all heavy atoms of the side chains in the QM region were allowed to move, except His496. All protons in the QM region were allowed to move, except 1HZ and 3HZ of Lys353, 2HH1 of Arg360, and HE2 of His404. The positions of these four protons had to be restrained due to interactions at the QM/MM interface. For Lys353 and His496, only the side chain was included in the QM region. The arginines required inclusion of the entire residue, backbone and side chain. Sample input files are available in the Supporting Information.

Results

Four Residue Calculations. Vanadate was modeled in the dianionic state with an axial hydroxo and three equatorial oxo moieties surrounded by three charged residues for these initial calculations. Vanadate, Lys353, Arg360, Arg490, and His496 were all included in the QM region (Figure 4a). The

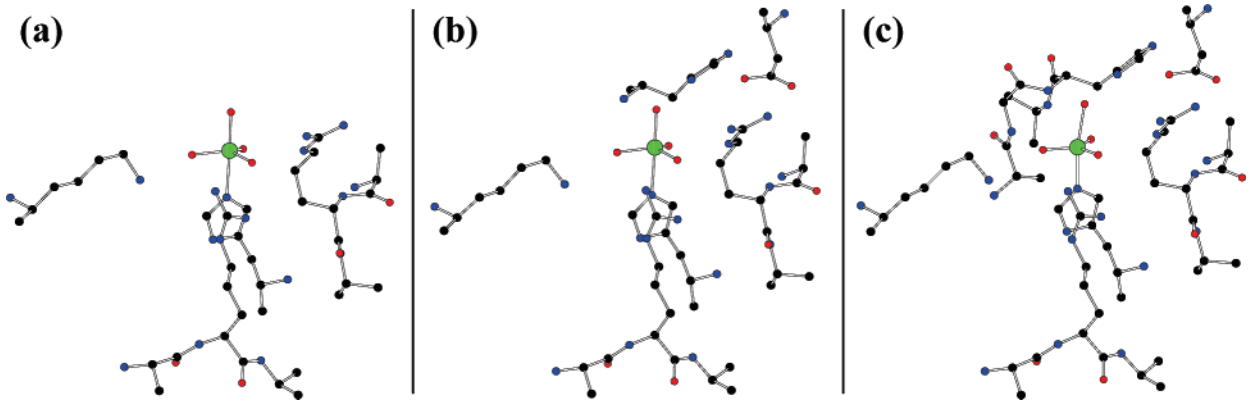

Figure 4. Residues in the QM region for (a) four residue, (b) six residue, and (c) full resting state and first protonated state calculations. For clarity, protons and the interfacial atoms have been omitted. It should be noted that a significant portion of the neighboring backbone atoms are required when including arginines in the QM region with QSite.

Table 1: For the Four Residue Calculations, the Energy Difference of $V(OH)O_3$ Surrounded by Three Cationic Neighbors versus the Transfer of a Proton from the Noted Residue to the Nearest Equatorial Oxygen on Vanadate[d]

deprotonated side chain	ΔE (kcal/mol)
3 cationic residues + $V(OH)O_3$	0
Lys353[a]	−2.8
Arg360[b]	5.3
Arg490η[b]	8.4
Arg490ϵ[c]	14.9

[a] Proton transferred to O1. [b] Proton transferred to O2. [c] Proton transferred to O3. [d] Negative values indicate that the proton transfer is favorable.

goal was to determine the protonation state of vanadate and the hydrogen-bonding scaffold. Our previous calculations of model systems indicated that the equatorial oxygens can abstract protons from neighboring cationic residues. Each of the three charged residues could donate a proton to the vanadate. There are two possible positions from which Arg490 could donate a proton: the terminal $\eta 2$ nitrogen (denoted 490η) or the ϵ nitrogen (denoted 490ϵ). Table 1 presents a series of calculations to examine proton placement. For each residue, we calculated the energy for the charged residue + $V(OH)O_3$ versus transferring the proton to an equatorial oxygen to produce a neutral residue + $V(OH)_2O_2$. Only the transfer of a proton from Lys353 to vanadate lowered the energy of the system. Combinations of transferring a second proton, in addition to the one from Lys353 to O1, were also examined. Upon minimization, a second proton on O2 or O3 simply transferred back to the appropriate arginine nitrogen.

Six Residue Calculations. As a second series of calculations, all four residues from the previous calculations, plus the side chains of Asp292 and His404, were included in the QM region (Figure 4b). This QM region had an overall neutral charge. The protonation states calculated in the four residue system were minimized in this larger, more complete system. The calculations were initiated with partial minimization where the heavy atoms of the side chains were held fixed, and then, the partial minima were refined with a second minimization where the side-chain heavy atoms were also unrestrained. At the point of freeing the side chains, it became necessary to constrain the positions of certain atoms at the QM/MM interface and His496. The ring atoms of His496 were constrained to the crystal structure positions, and the terminal protons of Lys353, proton 2HH1 from Arg360, and proton HE2 from His404 were constrained to remain fixed in positions taken from the minimum structure in which a proton from Lys353 has been transferred to the vanadate. Only two lysine protons were frozen, even in cases where there were three protons on the lysine, because all protons which interact directly with the vanadate were allowed to move freely in all minimizations.

In this series of calculations, transferring a proton from Lys353 to the vanadate is even more favorable by well over 7 kcal/mol. All other structures in which one or two protons are donated to vanadate are over 9 kcal/mol higher in energy than the global minimum. Contrary to the four residue calculations, structures where O2 or O3 are protonated, in addition to O1 being protonated by Lys353, were stable minima but high in energy (Table 2).

Table 2: For the Six Residue Calculations, Energy Difference of Transferring Protons from the Three Cationic Residues to Vanadate's Equatorial Oxygens

deprotonated side chain	ΔE (kcal/mol)
3 cationic residues + $V(OH)O_3$	0
Lys353[a]	−7.7
Arg360[b]	6.0
Arg490η[b]	2.8
Arg490ϵ[c]	1.9
Lys353 + Arg360[d]	14.1
Lys353 +Arg490η[d]	5.0
Lys353 + Arg490ϵ[e]	6.2

[a] Proton transferred to O1. [b] Proton transferred to O2. [c] Proton transferred to O3. [d] Protons transferred to O1 and O2. [e] Protons transferred to O1 and O3.

Full Resting State Calculations. In the calculations presented above, we have established that the dianionic form of the vanadate is not preferred in the active site. Instead, the anionic state is formed preferentially by abstracting a proton from Lys353. However, the small model calculations indicated that the residues in the active site were fully protonated in the resting state. Therefore, the next set of calculations included an additional proton in the active site, making the overall charge of the active site +1 (+1 from each Arg and Lys and −1 each from Asp and the anionic, doubly protonated vanadate). For completeness, we also examined structures in which the vanadate was singly protonated and the added proton was located on His404. To include His404 properly in the calculation, the entirety of His404 and Gly403 were required in the QM region (Figure 4c). Since the structure in which Lys353 donated a proton to vanadate was the previous global minimum, the coordinates for that structure served as the basis for this set of calculations, with the positions of the protons in the active site altered as needed. Four calculations were carried out in which Lys353 was in the free base form and O1 was protonated. In these calculations, the additional proton was added to O2, O3, the axial hydroxide, or His404. Five calculations were carried out based on the minimum with Lys353 protonated and the vanadate in the dianionic form. In these calculations, the additional proton was added to O1, O2, O3, the axial hydroxide, or His404.

Figure 5 shows the two lowest-energy structures in which Lys353 and O2 were protonated (Table 3b) or Lys353 was protonated and the axial position contained a water moiety (Table 3d). The difference in energy between these two structures was only a third of a kcal/mol, and both were ∼6 kcal/mol lower in energy than the next most favorable structure (Table 3c). The structures in which O1 and either Lys353 or His404 were protonated were the highest-energy structures (Table 3 (parts a and g, respectively)). In the first case, the proton on O1 was oriented away from Lys353 to minimize the repulsion between the two protons. In the second case, the proton of the axial hydroxo group was oriented away from His404 for the same reason. Adding a proton to O2 or O3 while O1 was protonated and Lys353 was in the free-base form resulted in the transfer of the O1

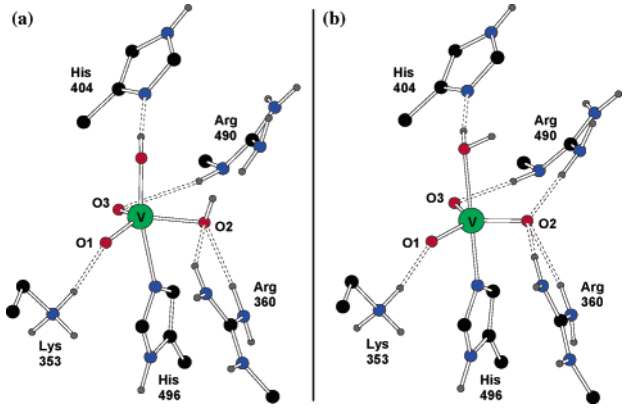

Figure 5. The two lowest-energy minima from the full resting state calculations. For clarity, many of the atoms in the QM region are not shown. (a) Minimum with axial and equatorial hydroxo groups and two equatorial oxo groups. (b) Minimum with an axial water and three equatorial oxo groups. In (a), a hydrogen bond exists from Arg490 to O2 as it does in (b), but it is not drawn in (a) so that the reader can better understand that the hydrogen on O2 points up toward the axial hydroxo. In (a), the axial O−V−O2−H atoms are nearly coplanar as are the equivalent O2−V−axial O−H atoms in (b).

Table 3: Relative Energies for Each Stable Minimum from the Full Resting State Calculations

structures with Lys353 protonated	ΔE (kcal/mol)
(a) O1 protonated	26.4
(b) O2 protonated	0
(c) O3 protonated	6.0
(d) axial water	0.3
(e) His404 protonated	18.1
structures with Lys353 deprotonated	**ΔE (kcal/mol)**
(f) O1 protonated and axial water	22.6
(g) O1 and His404 protonated	31.8

proton to Lys353 to produce structures similar to those in Table 3b,c. Protonation of the axial position does not result in transfer of the O1 proton to Lys353, but the structure is relatively high in energy (Table 3f). Schematic pictures and QM coordinates of each minimum listed in Table 3 may be found in the Supporting Information.

First Protonation State Calculations. The first step in the catalytic cycle is the protonation of one vanadate oxygen group.[7] It is not known which site is protonated in this first step. To determine this, we protonated each of the two minimum energy structures of the full resting state (Figure 5) in every possible location. These calculations were identical to the previous set of calculations except that the charge of the QM region was increased to +2 by the addition of the proton (Figure 4c).

The global minimum was the structure with an axial water and a protonated O3 (Table 4c and Figure 6). The next lowest-energy structure was 7 kcal/mol higher in energy (Table 4h), and O2 and His404 were protonated. All other structures are higher in energy by 20 kcal/mol or more (Table 4). Schematic pictures and QM coordinates of each minimum listed in Table 4 may be found in the Supporting Information.

Table 4: Relative Energy (in kcal/mol) for Each Stable Minimum from the First Protonation State Calculations

structures with axial water	ΔE vs axial water and O3 protonated
(a) O1 protonated	32.9
(b) O2 protonated	26.9
(c) O3 protonated	0
(d) His404 protonated	19.7
structures with axial hydroxide	**ΔE vs axial water and O3 protonated**
(e) O1 and O2 protonated	41.0
(f) O2 doubly protonated	44.0
(g) O2 and O3 protonated	37.9
(h) O2 and His404 protonated	7.1

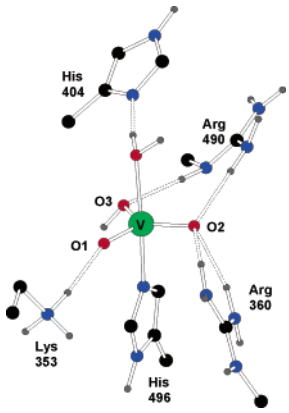

Figure 6. QM region of the global minimum from the first protonated state calculations. For clarity, not all the atoms in the QM region are shown.

Discussion

Enzymology,[11,50−52] synthetic model chemistry,[7,53−57] and small model calculations[1,2,25,58] have provided a wealth of information on the catalytic activity of the VCPOs. This study is the first application of QM/MM calculations to VCPOs which allows us to add additional atomic details to the understanding of the influence of the protein on the catalysis. We used this technique to describe more accurately the protonation states and interactions of the vanadate and surrounding residues of the active site.

The system setup was very carefully done to ensure that the electrostatic influence of the whole protein was unaltered in the truncated model. The truncated model provides the same topography of the potential surface, ensuring that wave functions would be influenced in nearly the same manner in the full and truncated systems. It should be stressed that similar comparisons should be done in any QM/MM calculation when the MM region must be truncated.

The QM region was built up in a systematic fashion to examine as many protonation states as possible, yet focus the most expensive calculations on the most likely states. The six residue calculations clearly showed that Lys353 is the only possible proton donor in the active site. This is logical because lysines have lower pK_as than arginines. The only other possibility was a protonated His404 playing the role of an acid, but the largest calculations all

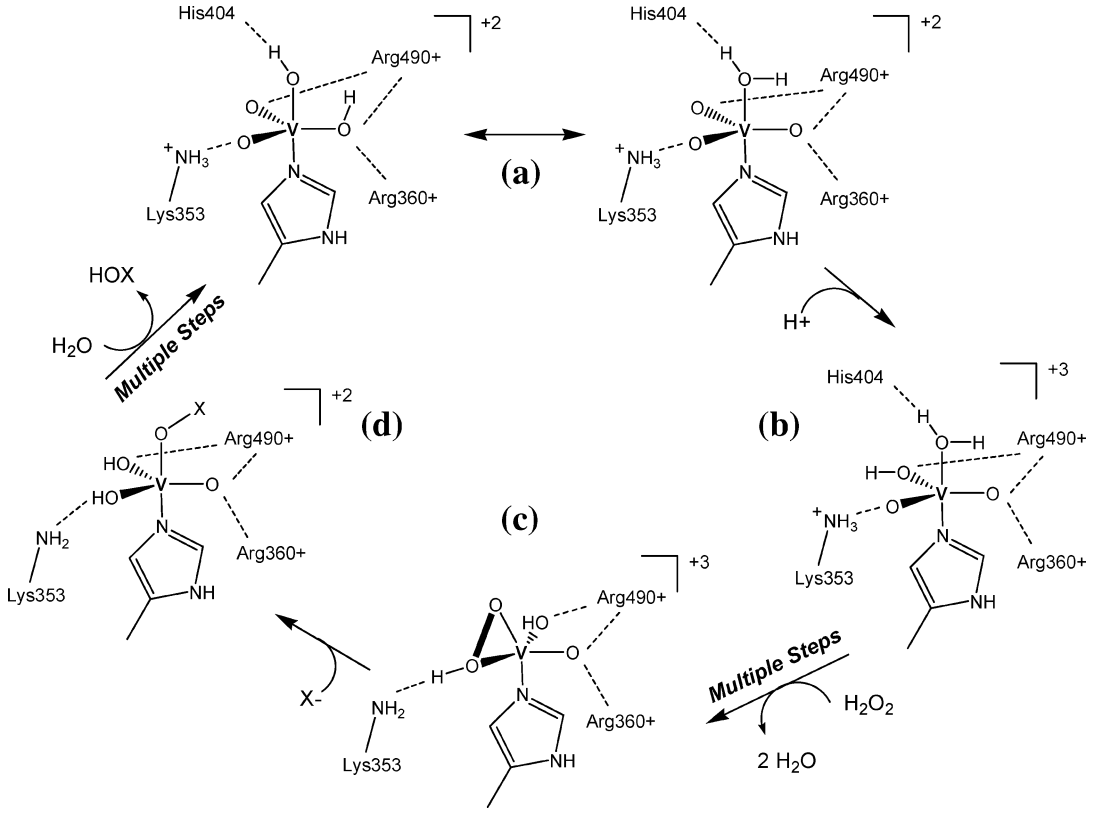

Figure 7. Proposed catalytic cycle based on the current and previous calculations. Panels (a) and (b) represent the minima calculated in this QM/MM study. Panels (c) and (d) represent minima calculated in other studies[2] combined with insights into the active site from our QM/MM calculations. Panel (a) is the hybrid of the two resting state configurations. Panel (b) is the first protonated state. Panel (c) represents the hydroperoxide-bound structure. Panel (d) represents the state in which the halide has been oxidized and is still bound to the vanadate.

show that His404 is not protonated in the resting or first protonated state.

Previously published small model calculations[1,2] suggest that the equatorial plane of the anionic vanadate should be surrounded by active-site residues which are all fully protonated. An additional proton was added to the calculation to provide the full resting state. Models with Lys353 in both the protonated and deprotonated states were examined. This resulted in nine calculations with the same large QM region in which we protonated the vanadate at each of the oxygens, including the axial position, and also at His404. In the systems with Lys353 neutral and O1 protonated, only two systems produced stable minima, but they were very high in energy. (Adding the proton to either O2 or O3 resulted in the O1 proton transferring back to Lys353.) We found that the protonation of Lys353 was overwhelmingly preferred over the double protonation of the equatorial plane of the vanadate. The results also show that when Lys353 is fully protonated, O1 is no longer the preferred position for the equatorial hydroxo group as might be expected. The most favorable equatorial position for protonation is at O2, which accepts hydrogen bonds from both arginines. The added proton on O2 is oriented up toward the axial hydroxo (Figure 5a). It is also highly favorable to protonate the axial position, resulting in an axial water. The added proton to create the axial water is oriented over O2 (Figure 5b). Both minima in Figure 5 show that the four atoms (O2−V−axial O−added proton) lay in a near-planar arrangement. When the two structures are overlaid, the positions of the added proton on the axial water vs O2 are only 2.2 Å apart. The proton can most likely tunnel between these two nearby locations. Because the two structures are nearly isoenergetic and easily interconverted, we propose a hybrid resting state, shown in Figure 7a.

Our previous small model calculations indicated that the sole structure of the resting state included two hydroxo groups, one in the axial position and one in the equatorial plane, likely at O1.[1,2] The more complete systems presented here refine the previous proposal on two accounts. First, this study shows that the resting state is comprised of not one but two structures. Second, they indicate that it is not the O1 position which is protonated but rather the O2 position. This may be surprising; after all, O2 is complemented by two arginines, while O1 and O3 only interact with one charged residue each. The electrostatic field of two Arg side chains should make O2 the least favorable site to protonate, but the reader is referred to Figure 2. When the full electrostatic field of the entire protein is calculated, one can see that the positive potential is actually weakest in the region of O2 and the axial hydroxo. It is reasonable for the proton to occupy the gap in the field between O2 and the axial position.

The strongest positive field is located at O1, and there is a very strong hydrogen bond between Lys353 and O1. Mutagenesis studies have shown that Lys353 is more important for catalysis than the arginines in the active site.[22]

The tight hydrogen bond from Lys353 to vanadate, coupled with the information from the mutagenesis studies, prompted us to propose an interesting catalytic role for Lys353 (more detail below).

Since the small molecule experiments of Colpas et al. showed that the first step in catalysis is the protonation of the vanadate,[59] we examined the first protonation state of the enzyme as well. Our previous small model calculations indicated that there were two structures in equilibrium in the protonated state. One included three hydroxo groups: one in the axial position and two in the equatorial plane. Our current, more complete calculations show that such a configuration is a stable minimum but much too high in energy to be relevant. The second minimum in the small model calculations contained a water moiety in the axial position and one hydroxo group in the equatorial plane. This QM/MM study shows that the later minimum is the lowest in energy, and O3 is the favorable position for the added proton in the first protonated state. Again, the long-range electrostatics can explain why O3 is the most favorable site for protonation. The position between O2 and the axial hydroxo is already occupied, and the highest positive potential in the active site is located at O1. When protonation occurs, O3 is the most favorable site to accept the proton. Upon protonation of O3, the hybrid form of the resting state appears to become biased toward the axial water configuration.

While this study has only quantified the resting state and first protonation state of the enzyme, it has laid the groundwork for the confirmation of the other intermediates proposed in this catalytic cycle, and we can propose a modified catalytic cycle (Figure 7). The calculations of the full resting state imply that it is a hybrid of the two lowest-energy minima (Figure 7a). In the first protonation state, O3 is protonated, and the hydrogen tunneling between the axial and O2 positions is localized on the axial position, creating a water molecule (Figure 7b).

In the next steps of the catalytic cycle, it is known that the incoming hydrogen peroxide displaces the axial water and one equatorial oxygen moiety (Figure 7c). The lowest unoccupied molecular orbital (LUMO) of the first protonation state shows that any electron density contributed to this orbital by the attacking peroxide would weaken and lengthen the bonds between the vanadium and the equatorial oxo groups (Figure 8). A longer, weaker oxo bond would be more basic, making it very likely that O1 abstracts a proton from Lys353. We propose that O1 is the second oxygen moiety which is displaced (quite possibly leaving as a water molecule after a second protonation by the hydrogen peroxide). Previous computational studies of model systems indicate that the equatorial hydroperoxide oxygen is one which is protonated.[2] This group would favorably donate a hydrogen bond to the resulting free-base form of Lys353 (as shown in Figure 7c). Furthermore, both computational studies and the crystal structure of the peroxide-bound form[21] indicate a strong hydrogen bond between Lys353 and the equatorially bound peroxide oxygen.

The halide can then attack the pseudoaxial hydroperoxide oxygen (Figure 7d), as indicated by the study by Zampella et al.[2] A protein-bound water molecule or the O3 equatorial hydroxide could then protonate the axial OX^-, making it a better leaving group. The HOX species is displaced. Transfer of a proton from the former equatorial hydroperoxide oxygen back to Lys353 reforms the resting state (Figure 7a).

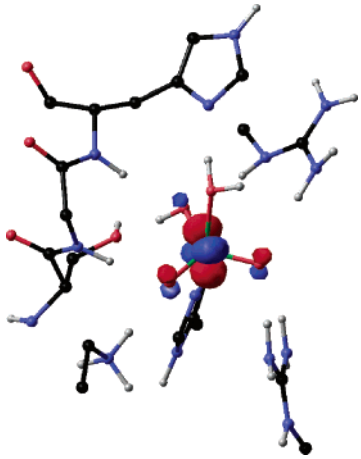

Figure 8. The LUMO of the first protonation state is shown with a cutoff of −0.100. The LUMO is made up of an antibonding orbital between vanadium and primarily the two oxo groups, with minor contribution from the hydroxo group. We found that the HOMO is simply the lone pair on His404 that accepts a hydrogen bond from the axial water (data not shown).

The crystal structure of the peroxide bound form[21] was interpreted as having the hydroxo group located at O2, not O3 as we are proposing. The crystal structure was not of high enough resolution to identify positions of hydrogens, and the uncertainty in atomic positions makes it very speculative to differentiate between an oxo and hydroxo bond length. Questions about the catalytic steps and protonation states of the next intermediates could be answered by carrying out QM/MM calculations of the later stages in the catalytic cycle. There are multiple steps between parts b and c of Figure 7 as well as between parts c and d of Figure 7. Computational studies are one of a few ways to gain insights into such fleeting and reactive states.

Conclusions

We have used QM/MM calculations to refine the resting state and first protonation state of the vanadium dependent chloroperoxidase. We have shown how the LUMO of the first protonated state and the strong hydrogen bond between Lys353 and O1 support a modification of the catalytic cycle.

Our previous small model calculations predicted that an anionic vanadate unit with one hydroxo group in the equatorial position and a second in the equatorial plane would be most favorable. These calculations support that prediction and add new information by indicating O2 as the likely position of the equatorial hydroxo group in the resting state. The calculations also reveal that an anionic vanadate with an axial water, which was not stable in the small model calculations, is actually very stable in the protein environment and is nearly isoenergetic with the previously proposed resting state. Our current calculations suggest that the resting state is actually a hybrid of these two minima, with the

configuration containing an axial water being more important for generating the first protonated state. Our previous small model calculations indicated that there were two structures that were nearly isoenergetic upon protonation of the active site. However, these QM/MM calculations reveal only one low-energy minimum with an axial water and an equatorial hydroxo group at O3. The influence of long-range electrostatics in this system appears to significantly influence the most favorable positions for protonation. These findings highlight the importance of incorporating the protein environment into quantum mechanical models of protein active sites.

Acknowledgment. The authors appreciate the generosity of Prof. William L. Jorgensen and Dr. D. C. Lim for their donation of the ChemEdit software which was used to make several figures in this paper. We thank the following agencies for support of this work: Beckman Young Investigator Program (H.A.C.), NIH GM42703 (V.L.P.), and NIH GM008270 Michigan Molecular Biophysics Training Grant (J.Y.K.). We would also like to thank Dale Braden and Jeff Saunders of Schrödinger, Inc. for helpful conversations and Dr. Anna Bowman for her help with the figures.

Supporting Information Available: A list of residues included in the truncated protein model; sample input files for QM/MM calculations; and schematic pictures, energies, and QM coordinates for all minima from the full resting state and first protonated state calculations. This material is available free of charge via the Internet at http://pubs.acs.org.

References

(1) Zampella, G.; Kravitz, J. Y.; Webster, C. E.; Fantucci, P.; Hall, M. B.; Carlson, H. A.; Pecoraro, V. L.; De Gioia, L. *Inorg. Chem.* **2004**, *43*, 4127−4136.

(2) Zampella, G.; Fantucci, P.; Pecoraro, V. L.; De Gioia, L. *J. Am. Chem. Soc.* **2005**, *127*, 953−960.

(3) Everett, R. R.; Butler, A. *Inorg. Chem.* **1989**, *28*, 393−395.

(4) van Schijndel, J. W. P. M.; Barnett, P.; Roelse, J.; Vollenbroek, E. G. M.; Wever, R. *Eur. J. Biochem.* **1994**, *225*, 151−157.

(5) Butler, A. *Coord. Chem. Rev.* **1999**, *187*, 17−35.

(6) de Boer, E.; Tromp, M. G. M.; Plat, H.; Krenn, G. E.; Wever, R. *Biochim. Biophys. Acta* **1986**, *872*, 104−115.

(7) Colpas, G. J.; Hamstra, B. J.; Kampf, J. W.; Pecoraro, V. L. *J. Am. Chem. Soc.* **1996**, *118*, 3469−3478.

(8) de la Rosa, R. I.; Clague, M. J.; Butler, A. *J. Am. Chem. Soc.* **1992**, *114*, 760−761.

(9) Martinez, J. S.; Carrol, G. L.; Tschirret-Guth, R. A.; Altenhoff, G.; Little, R. D.; Butler, A. *J. Am. Chem. Soc.* **2001**, *123*, 3289−3294.

(10) Wever, R.; Kustin, K. In *Advances in Inorganic Chemistry*; Sykes, A. G., Ed.; Academic Press: New York, 1990; Vol. 35, pp 103−137.

(11) Carter-Franklin, J. N.; Butler, A. *J. Am. Chem. Soc.* **2004**, *126*, 15060−15066.

(12) Everett, R. R.; Soedjak, H. S.; Butler, A. *J. Biol. Chem.* **1990**, *265*, 15671−15679.

(13) ten Brink, H. B.; Tuynman, A.; Dekker, H. L.; Hemrika, W.; Izumi, Y.; Oshiro, T.; Schoemaker, H. E.; Wever, R. *Inorg. Chem.* **1998**, *37*, 6780−6784.

(14) Smith, T. S., II; Pecoraro, V. L. *Inorg. Chem.* **2002**, *41*, 6754−6760.

(15) Conte, V.; Di Furia, F.; Modena, G. *J. Org. Chem.* **1988**, *53*, 1165−1669.

(16) Butler, A.; Clague, M. J.; Meister, G. E. *Chem. Rev.* **1994**, *94*, 625−638.

(17) Bortolini, O.; Di Furia, F.; Scrimin, P.; Modena, G. *Nouv. J. Chim.* **1985**, *9*, 147−150.

(18) Mimoun, H.; Saussine, L.; Daire, E.; Postel, M.; Fischer, J.; Weiss, R. *J. Am. Chem. Soc.* **1983**, *105*, 3101−3110.

(19) Sheldon, R. A.; Kochi, J. K. *Metal-catalyzed oxidations of organic compounds: mechanistic principles and synthetic methodology including biochemical processes*; Academic Press: New York, 1981.

(20) Ligtenbarg, A. G. J. In *Chemistry*; University of Groningen: Groningen, Holland, 2001.

(21) Messerschmidt, A.; Prade, L.; Wever, R. *Biol. Chem.* **1997**, *378*, 309−315.

(22) Hemrika, W.; Renirie, R.; Macedo-Ribeiro, S.; Messerschmidt, A.; Wever, R. *J. Biol. Chem.* **1999**, *274*, 23820−23827.

(23) Macedo-Ribeiro, S.; Hemrika, W.; Renirie, R.; Wever, R.; Messerschmidt, A. *J. Biol. Inorg. Chem.* **1999**, *4*, 545−559.

(24) Buhl, M. *Angew. Chem., Int. Ed* **1998**, *37*, 142−144.

(25) Buhl, M. *J. Comput. Chem.* **1999**, *20*, 1254−1261.

(26) Buhl, M.; Hamprecht, F. A. *J. Comput. Chem.* **1998**, *19*, 113−122.

(27) Buhl, M.; Parrinello, M. *Chem. Eur. J.* **2001**, *7*, 4487−4494.

(28) Conte, V.; Di Furia, F.; Moro, S. *J. Mol. Catal. A* **1997**, *117*, 139−149.

(29) Bortolini, O.; Carraro, M.; Conte, V.; Moro, S. *Eur. J. Biochem.* **2003**, 42−46.

(30) Conte, V.; Di Furia, F.; Moro, S.; Rabbolini, S. *J. Mol. Catal. A* **1996**, *113*, 175−184.

(31) Messerschmidt, A.; Wever, R. *Proc. Natl. Acad. Sci. U.S.A.* **1996**, *93*, 392−396.

(32) Philipp, D. M.; Friesner, R. A. *J. Comput. Chem.* **1999**, *20*, 1468−1494.

(33) Murphy, R. B.; Philipp, D. M.; Friesner, R. A. *J. Comput. Chem.* **2000**, *21*, 1442−1457.

(34) Murphy, R. B.; Philipp, D. M.; Friesner, R. A. *Chem. Phys. Lett.* **2000**, *321*, 113−120.

(35) Wirstam, M.; Lippard, S. J.; Friesner, R. A. *J. Am. Chem. Soc.* **2003**, *125*, 3980−3987.

(36) Guallar, V.; Baik, M.-H.; Lippard, S. J.; Friesner, R. A. *Proc. Natl. Acad. Sci. U.S.A.* **2003**, *100*, 6998−7002.

(37) QSite 2.5 revision 20, Schrodinger, LLC, New York City, 2003.

(38) Jorgensen, W. L.; Maxwell, D. S.; Tirado-Rives, J. *J. Am. Chem. Soc.* **1996**, *118*, 11225−11236.

(39) Becke, A. D. *J. Chem. Phys.* **1993**, *98*, 5648−5652.

(40) Lee, C.; Yang, W.; Parr, R. G. *Phys. Rev. B* **1988**, *37*, 785−789.

(41) Hay, P. J.; Wadt, W. R. *J. Chem. Phys.* **1985**, *82*, 299−310.

(42) Ditchfield, R.; Hehre, W. J.; Pople, J. A. *J. Chem. Phys.* **1971**, *54*, 724−728.

(43) Hehre, W. J.; Ditchfield, R.; Pople, J. A. *J. Chem. Phys.* **1972**, *56*, 2257−2261.

(44) Hehre, W. J.; Pople, J. A. *J. Chem. Phys.* **1972**, *56*, 4233−4234.

(45) Binkley, J. S.; Pople, J. A. *J. Chem. Phys.* **1977**, *66*, 879−880.

(46) Francl, M. M.; Pietro, W. J.; Hehre, W. J.; Binkley, J. S.; Gordon, M. S.; DeFrees, D. J.; Pople, J. A. *J. Chem. Phys.* **1982**, *77*, 3654−3665.

(47) Hariharan, P. C.; Pople, J. A. *Theor. Chim. Acta* **1973**, *28*, 213−222.

(48) Molecular Operating Environment, Chemical Computing Group, Inc., Montreal, Quebec, Canada, 2002.

(49) Impact 2.5 revision 20, Schrodinger, LLC, New York City, 2003.

(50) de Boer, E.; Wever, R. *J. Biol. Chem.* **1988**, *263*, 12326−12332.

(51) Carter, J. N.; Beatty, K. E.; Simpson, M. T.; Butler, A. *J. Inorg. Biochem.* **2002**, *91*, 59−69.

(52) Casny, M.; Rehder, D.; Schmidt, H.; Vilter, H.; Conte, V. *J. Inorg. Biochem.* **2000**, *80*, 157−160.

(53) Colpas, G. J.; Hamstra, B. J.; Kampf, J. W.; Pecoraro, V. L. *J. Am. Chem. Soc.* **1994**, *116*, 3627−3628.

(54) Colpas, G. J.; Hamstra, B. J.; Kampf, J. W.; Pecoraro, V. L. *Inorg. Chem.* **1994**, *33*, 4669−4675.

(55) Andersson, M.; Conte, V.; Di Furia, F.; Moro, S. *Tetrahedron Lett.* **1995**, *36*, 2675−2678.

(56) Bortolini, O.; Carraro, M.; Conte, V.; Moro, S. *Eur. J. Biochem.* **1999**, 1489−1495.

(57) Clague, M. J.; Keder, N. L.; Butler, A. *Inorg. Chem.* **1993**, *32*, 4754−4761.

(58) Conte, V.; Bortolini, O.; Carraro, S.; Moro, S. *J. Inorg. Biochem.* **2000**, *80*, 41−49.

(59) Colpas, G. J.; Hamstra, B. J.; Kampf, J. W.; Pecoraro, V. L. *J. Am. Chem. Soc.* **1996**, *118*, 3469−3478.

CT050132O